REAL-TIME REFRACTIVITY RETRIEVAL USING THE MAGNETRON-BASED CASA X-BAND RADAR NETWORK DURING THE SPRING 2008 CAMPAIGN

B. L. Cheong[1], R. Palmer[1], V. Chandrasekar[2], F. Junyent[2]

[1] Atmospheric Radar Research Center, and School of Meteorology, University of Oklahoma
[2] Department of Electrical and Computer Engineering, Colorado State University

ABSTRACT

A real-time refractivity retrieval platform for the CASA IP-1 [1] testbed is currently being developed at the University of Oklahoma. From our previous efforts in the 2007-2008 KTLX/KFDR refractivity experiment [2], a software module to produce refractivity products has been developed and is ported over to the IP-1 testbed this year. One of the challenges for refractivity using the IP-1 radars is the use of X-band systems, which results in more rapid phase wrapping across ranges. In this work, a theoretical explanation will be presented to show that X-band is not a limiting factor to refractivity retrieval. Another significant challenge is the use of magnetron-based transmitter, which changes the effective wavelength being applied for measuring the propagation phase. This question remains open but it will be shown that through the use of differential refractivity technique, scan-to-scan refractivity can still be useful in practice.

Index Terms— Surface Refractivity, X-band magnetron radars, CASA, IP-1 radars.

1. INTRODUCTION

Radar refractivity retrieval has received increasing attention recently as a possible additional radar product to the standard reflectivity, radial velocity and spectrum width that are currently produced by most radars, e.g., WSR-88D. Based on the radar refractivity retrieval concepts found in the work by [3], a real-time refractivity processing platform has been implemented at the University of Oklahoma (OU) and has been successfully applied on the KTLX and KFDR WSR-88D radar during the Spring of 2007 and 2008 [2]. The technique relies on the returned phase from ground clutter, which changes according to the refractivity of the atmosphere and by using the phase, a refractivity field is reconstructed.

There are at least two significant complications for X-band magnetron-based radars for refractivity application. First, the shorter wavelength being used increases the so-called phase-wrapping rate, which makes subsequent processing steps problematic. Second, magnetrons inherently exhibit frequency drift that prevents the two radar scans from sharing the same frequency (wavelength), which makes deriving the refractivity change over two scans difficult.

In this paper, a theory to show that CASA IP-1 radars do not suffer from the use of X-band in radar refractivity retrieval will be presented. Then, the *Differential Refractivity* (DRR) technique will be presented to show it mitigates the frequency drift complication from the magnetron of the IP-1 radars for scan-to-scan retrieval. Finally, a real-time refractivity platform design for the IP-1 testbed will be discussed.

2. REFRACTIVITY FOR MAGNETRON X-BAND

The received phase from stationary targets is a path-integrated function of the refractive index, which can be described as follows

$$\phi(r) = -\frac{4\pi f}{c}\int_0^r n(\gamma)d\gamma \tag{1}$$

where f represents the frequency, c represents the speed of light (299,792,458 $\mathrm{m\,s^{-1}}$) and r is the range. With the radar wavelength on the order of cm and $n \approx 1$, the measured phase wraps many times within a resolution volume depth which makes deriving refractivity directly from a single scan (Equation (1)) impossible. To mitigate this phase wrapping problem, [3] proposed that the change of refractivity between two scans can be obtained instead, i.e.,

$$\begin{aligned}\Delta\phi(r) &= \phi(r,t_1) - \phi(r,t_0) \\ &= -\frac{4\pi f}{c}\int_0^r \left[n(\gamma,t_1) - n(\gamma,t_0)\right] d\gamma. \end{aligned} \tag{2}$$

By performing a derivative operator on both sides of (2), and using the definition of refractivity $N = 10^{-6}(n-1)$, one can show that refractivity is a function of phase change as follows

$$\begin{aligned}\Delta N &= -10^6\left[n(r,t_1) - n(r,t_0)\right] \\ &= -10^6 \frac{c}{4\pi f}\frac{d}{dr}\left[\phi(r,t_1) - \phi(r,t_0)\right] \end{aligned} \tag{3}$$

The term ΔN is expected to be noisy due to the mathematical characteristics of the derivative operator. In our experience, the standard deviation of this field can exceed 3 N-units. Therefore, it is subsequently smoothed to reduce the noisiness of this quantity. Absolute refractivity can be derived by adding the reference refractivity map to the difference, if desired.

2.1. Differential Refractivity Retrieval

To mitigate the rapid phase wrapping problem, we have proposed an algorithm called DRR, which accumulates refractivity differences between scans rather than over a longer time period, as is currently the practice. As a result, typical atmospheric changes over such a short time (less than 5 min apart) do not cause a significant change in signal phase, minimizing phase wrapping. A drawback of this technique is that estimation error/bias can accumulate over time leading to divergence of the estimate away from the true values. Subsequently, we discovered that DRR is not necessary for X-band applications with good range resolution. However, DRR is still useful for magnetron-based systems and this discussion will resume later in this paper. In the next section, a mathematical explanation will be presented to show that X-band suffers little if any performance lost in refractivity retrieval.

2.2. X-band

Using X-band radars in comparison to S-band, the shorter wavelength introduces a more rapid phase wrapping in the map of phase difference (refer to (2)). It was speculated that the subsequent processing will fail when phase wrapping is too rapid. Referring back to the refractivity retrieval procedure in (3), the radial derivative is calculated, in practice, as a phase difference (in 2π-modulo) on a gate-to-gate basis. So, (3) is applied as (4)

$$\Delta N = -10^6 \frac{c}{4\pi f} \frac{\Delta}{\Delta r} \left[\phi(r,t_1) - \phi(r,t_0)\right] \tag{4}$$

At a given discrete sampling interval in range (Δr), the accuracy of the derivative term is limited by how well the derivative is approximated by the finite difference in (4). As such, the maximum unambiguous estimate of the gradient of the phase difference term $\Delta[\phi(r,t_1) - \phi(r,t_0)]/\Delta r$ is limited to $\pm\pi/\Delta r$, which can be shown to have a maximum unambiguous refractivity difference as in (5) [4]

$$\Delta N_a = \pm 10^6 \frac{c}{4 f \Delta r} \tag{5}$$

We refer the above limit as the aliasing refractivity. Note that for higher operating frequency, the aliasing refractivity is reduced. However, the limit is also *improved* using a smaller gate sampling. For numerical comparisons, the WSR-88D radars use $f = 2.8\,\text{GHz}$ ($2.7 - 2.9\,\text{GHz}$) and $\Delta r = 250\ m$, that gives $N_a = 107\,$N-units ($103 - 111\,$N). For IP-1, on the other hand, with $f = 9.41\,\text{GHz}$ and $\Delta r = 96\ m$, $N_a = 83\,$N-units. It must be emphasized here that CASA IP-1 radars are capable of sampling up to $\Delta_r = 48\ m$, which results in $N_a = 166\,$N-units. Therefore, there is no penalty but a gain in N_a.

2.3. Magnetron

Another complication from using the the IP-1 radars is the frequency drift of the magnetron oscillator. During the REFRACTT-2006 campaign, the mobile XPOL radar from University of Massachusetts was used for initial test of refractivity retrieval using an X-band radar. At that time, the effects of frequency drifts on the refractivity retrieval algorithm were not well understood. Therefore, raw phase measurements and the frequency of the magnetron were monitored and stored in the hope of re-processing the data later in order to account for the effects induced by the drifting frequency.

Later, however, we learned that even *without* correction of frequency drift, the estimates of refractivity change were satisfactory when compared with the surface measurements. To resolve this issue, we formulated the procedure of retrieving refractivity with frequency drifts, which can be described as (6)

Due the frequency drift of the magnetron, additional phase offsets are introduced from time t_0 to time t_1 at the phase measurements. Here, we represent the phase offsets as $\phi_{\Delta f}$ and ϕ_ϵ in (6). Note that the amount of phase offset due to frequency drift are close to each other for range bins $(r - \Delta r)$ and r. That is, range bin $(r - \Delta r)$ and r both have the total phase offsets of $\phi_{\Delta f}$ and $\phi_{\Delta f} + \phi_\epsilon$, respectively. As such $\phi_{\Delta f}$ cancels due to the derivative operator in the refractivity algorithm and we are left with the residual term ϕ_ϵ, which is small and insignificant for the DRR method. This residual phase offset can be described mathematically as

$$\epsilon_\phi = -\frac{4\pi\Delta f}{c}\Delta r. \tag{8}$$

An example of the frequency drift behavior of the magnetron from an IP-1 radar is shown in Figure 1. One can see that most

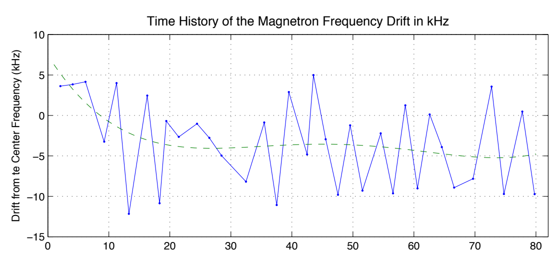

Fig. 1. A typical frequency drift of the magnetron from the KLWE IP-1 radar is not severe as the transmit components are housed inside a temperature-conditioned environment.

of the drift amounts are below 10 kHz. At this rate of $\Delta f = 10^3\,\text{Hz}$, $\Delta r = 96\,\text{m}$ and $\lambda = 0.03\,\text{m}$, the resultant phase error is merely 0.04 rad (2.3°), which is much less than the typical measurement noise. That explains why refractivity from DRR was still in agreement with the surface measurements from radiosonde even without any compensation for the frequency drift.

$$\frac{d}{dr}\left[\phi(t_1) - \phi(t_0)\right] \rightarrow \frac{1}{\Delta r}\left\{\left[\phi_{t_1}(r) - \phi_{t_0}(r) + \phi_{\Delta f} + \phi_{\epsilon}\right] - \left[\phi_{t_1}(r - \Delta r) - \phi_{t_0}(r - \Delta r) + \phi_{\Delta f}\right]\right\} \tag{6}$$

$$= \frac{1}{\Delta r}\left\{\left[\phi_{t_1}(r) - \phi_{t_0}(r) + \phi_{\epsilon}\right] - \left[\phi_{t_1}(r - \Delta r) - \phi_{t_0}(r - \Delta r)\right]\right\} \tag{7}$$

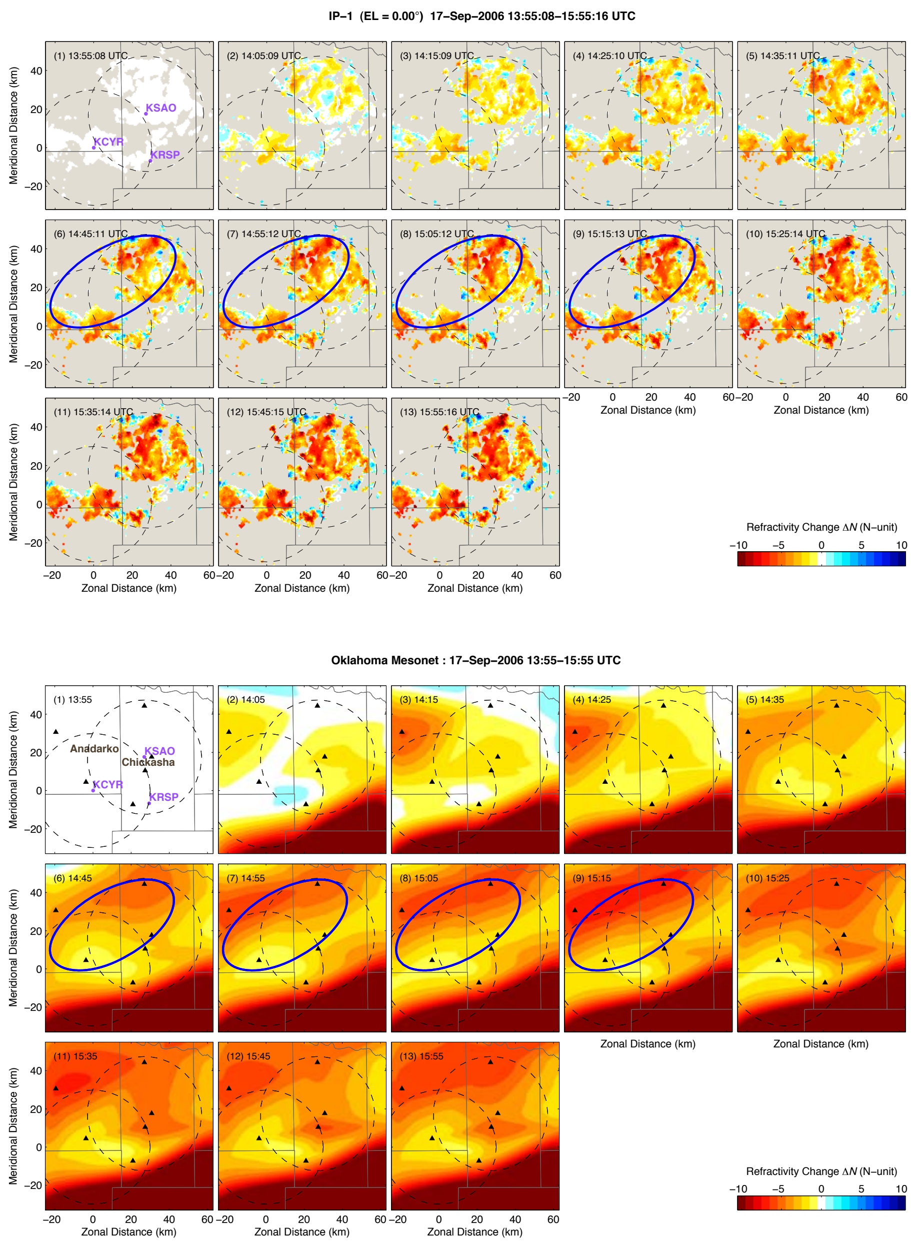

Fig. 2. Total refractivity change (13:55-15:55 UTC with 13:55 UTC as the reference) using measurements from the CASA IP-1 network and surface measurements from the Oklahoma Mesonet. It should be noted that general agreement is observed and, that by using the DRR method, frequency drift effects are minimized.

3. POTENTIAL RESULTS FROM IP-1 NETWORK

A time-series dataset was collected on September 17, 2006 with the CASA IP-1 network. Using the 2-hour contiguous data with two radars operating simultaneously from 13:55 to 15:55 UTC, we investigated the performance of the DRR without frequency drift compensation. During this time period, a weak storm was passing from the west of the domain. Differential refractivity fields are accumulated for the total change of refractivity since 13:55 UTC and is shown in the time history plot in the top half of Figure 2. The same quantity is derived from the surface measurements of the Oklahoma Mesonet and is shown in the bottom half of Figure 2.

From this comparison, one can see a qualitative agreement between the measurements from IP-1 network and Oklahoma Mesonet during this 2-hour period. More importantly, an apparent spatial structure annotated in ovals can be seen from both measurements. With this comparison, we can see the potential of retrieving refractivity using the CASA IP-1 network.

4. REAL-TIME DATA PROCESSING FOR IP-1 RADARS

Real-time processing software for radar refractivity has been developed here at OU. It is designed in a modular architecture for portability. That is, the same software module can be applied to different radars with minimal changes. Here at OU, we are planning to use the same software module for refractivity for seven radars, including the four CASA IP-1 radars. At the present time, we are finalizing the software between the IP-1 radars and the refractivity module.

The data flow from the raw I/Q time series to the fully processed radar products is shown in Figure 3. This design is currently being implemented. Since the spring of 2008, the IP-1 radars have started to collect phase measurements for refractivity retrieval. During the clear-air scans, the ground clutter filter is turned off and a field of phase estimates are measured from this scan as an additional product to the existing Level II data collection. Using the Local Data Manager (LDM) developed by Unidata, the Level II products are conveyed through the internet and ingested into a central processing node at the National Weather Center (NWC). After the refractivity products are generated, they are delivered to a Warning Decision Support System - Integrated Information (WDSS-II,[5]) data server, which stores and serves the radar products. Finally, the radar products are presented to end users via WDSS-II display software, which can be installed on multiple machines that are connected to the server to retrieve the radar products.

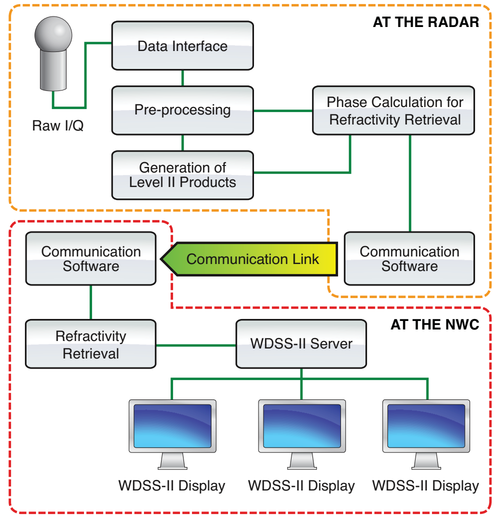

Fig. 3. Overview of data flow. In 2008, phase measurements have been added as Level II products from all the IP-1 nodes.

5. FUTURE PLANS

As mentioned earlier, the real-time platform is near completion. We are currently finalizing the software development and plan to start collecting X-band refractivity data for extended periods of time. With that dataset, we will investigate the effect of error propagation using the DRR method and assess the long-term robustness of radar refractivity retrieval using the CASA IP-1 radars.

6. REFERENCES

[1] F. Junyent, L. Krnan, M. Zink, V. Chandrasekar, and D. J. McLaughlin, "A reconfigurable weather radar network: Architecture, data flow, and preliminary observations," in *IGARSS 2006*, Denver, Colorado, July 2006.

[2] P. L. Heinselman, B. L. Cheong, R. D. Palmer, D. Bodine, and K. Hondl, "KTLX spring 2007 and 2008 refractivity experiment," *Wea. Forecasting*, vol. to be submitted, 2008.

[3] F. Fabry, C. Frush, I. Zawadzki, and A. Kilambi, "On the extraction of near-surface index of refraction using radar phase measurements from ground targets," *J. Atmos. Oceanic Technol.*, vol. 14, no. 4, pp. 978–987, August 1997.

[4] B. L. Cheong, R. D. Palmer, C. D. Curtis, T.-Y. Yu, D. S. Zrnić, and D. Forsyth, "Refractivity retrieval using the Phased Array Radar: First results and potential for multi-function operation," *IEEE Trans. Geosci. Remote Sens.*, vol. accepted, 2008.

[5] V. Lakshmanan, T. Smith, G. J. Stumpf, and K. Hondl, "The Warning Decision Support System - Integrated Information (WDSS-II)," *Weather and Forecasting*, vol. in press, 2006.